

Analysis of Meson Exchange and Isobar Currents in (e,e'p) Reactions from ^{16}O

J.E. Amaro and A.M. Lallena

Departamento de Física Moderna, Universidad de Granada, E-18071 Granada, Spain

J.A. Caballero

Departamento de Física Atómica, Molecular y Nuclear, Universidad de Sevilla, Apdo. 1065, E-41080 Sevilla, Spain

§

Instituto de Estructura de la Materia, CSIC, Serrano 123, E-28006 Madrid, Spain

An analysis of the effects of meson exchange and isobar currents in exclusive (e,e'p) processes from ^{16}O under quasi-free kinematics is presented. A model that has probed its feasibility for inclusive quasi-elastic (e,e') processes is considered. Sensitivity to final state interactions between the outgoing proton and the residual nucleus is discussed by comparing the results obtained with phenomenological optical potentials and a continuum nuclear shell-model calculation. The contribution of the meson-exchange and isobar currents to the response functions is evaluated and compared to previous calculations, which differ notably from our results. These two-body contributions cannot solve the puzzle of the simultaneous description of the different responses experimentally separated.

©1999 by The American Physical Society

PACS number: 25.30.Fj; 25.30.Rw; 24.10.-i; 21.60.Cs

Keywords: meson exchange currents; isobar currents; electromagnetic nucleon knockout; final state interactions; continuum shell-model; optical potential; structure response functions.

Electron scattering reactions have been widely used for a long time as one of the most powerful tools to probe nuclear structure. In particular, coincidence (e,e'p) reactions under quasifree kinematics are expected to yield details on electromagnetic properties of the nucleons inside the nucleus. Information about single-particle wave functions, spectroscopic factors and strength distributions can be extracted from the analysis of this type of processes [1]. However, such information is not completely free from ambiguities because of our still inaccurate knowledge of the mechanism of the reaction.

The simplest framework used to analyze (e,e'p) processes corresponds to the Born approximation with the nuclear current assumed to be given simply by the sum of the one-body currents from the individual nucleons (impulse approximation) and the electrons and outgoing proton treated as plane waves. This is obviously an oversimplified description of the reaction mechanism. Various additional ingredients aiming to provide a more complete description of the different aspects of the reaction should be included. Coulomb distortion of the electrons [2]- [4], final state interactions (FSI) of the emitted proton with the residual nucleus [3]- [5] and meson-exchange (MEC) and isobar (IC) currents [6]- [8], may have important effects and have been already reported in the literature using different approaches.

From the experimental point of view, the advent of continuous beam electron accelerators, together with the availability of polarized beams and targets as well as recoil polarimetry, have permitted the study of the nucleus in a wide kinematical range with a great resolution and precision.

In this work our interest is focused on the role played by the MEC and IC and their interplay with FSI. In particular, we investigate how these mechanisms affect to the five nuclear response functions that contribute to the $(\vec{e},e'p)$ cross section and which are directly related to the longitudinal and transverse parts of the nuclear electromagnetic operators. These responses have been measured recently for ^{16}O [9,10]. The data obtained for the longitudinal-transverse interference response in both experiments show an important discrepancy in the case of the $1p_{3/2}^{-1}$ hole state. This observation may require further experimental confirmation.

A theoretical evaluation of MEC and IC in coincidence (e,e'p) reactions, in particular for the longitudinal-transverse response, has been only presented in two previous works [7,8].

In Ref. [7], FSI were included within various non-relativistic phenomenological optical potentials and the evaluation of the two-body matrix elements was done in an approximate way by introducing an effective one-body current. In Ref. [8] the bound and continuum single-particle states correspond to Hartree-Fock wave functions. FSI are taken into account by means of a continuum RPA calculation and the evaluation of the matrix elements of the two-body current operators is done without approximations. The results obtained in both calculations differ notably, especially in the case of the longitudinal-transverse interference response. Whereas the authors in Ref. [7] predict a small contribution of MEC with an overall reduction of the response due to IC, the authors in Ref. [8] obtain important effects of both MEC and IC and a great enhancement of the interference response for the $1p_{3/2}^{-1}$ hole with respect to the $1p_{1/2}^{-1}$ one. The extent to which the differences in the respective models are responsible for the discrepancies in the results is still not clear.

Our purpose in this work is trying to shed some light on this problem. In order to do that we use a different approach that has proved to be very successful in the analysis of MEC and IC for inclusive (e,e') responses in the quasi-elastic peak [11]. This model has been also used to study other effects in quasi free electron scattering from nuclei (e.g., finite size effects [11,12], and relativistic corrections, polarization degrees of freedom and parity violation [12,13]) and the width of the radiative pion capture by nuclei [14]. We present calculations for proton knockout off ^{16}O from the $1p_{1/2}$ and $1p_{3/2}$ orbits and compare them to the corresponding data reported in Ref. [10] for values of the momentum transfer and excitation energy of 460 MeV/c and 100 MeV, respectively. It is important to point out that in our calculation all the matrix elements of the two-body currents are evaluated without approximations. Thus, we avoid the reduction performed in Ref. [7] treating much better the nuclear structure problem. On the other hand, FSI are accounted for by means of phenomenological complex optical potentials which permit to include flux losses to more complicated configurations, something that is not considered in Ref. [8].

The general formalism for ($\bar{e},e'p$) reactions has been presented in detail in several previous papers [1,13,15]. Assuming plane waves for the electron (treated in the extreme relativistic limit) and parity conservation, the cross section in Born approximation can be written as:

$$\left(\frac{d\sigma}{d\varepsilon'd\Omega'd\Omega_p}\right)^h = \kappa\sigma_M \left[\tilde{v}_L W^L + \tilde{v}_T W^T + \tilde{v}_{TL} W^{TL} \cos\phi_p + \tilde{v}_{TT} W^{TT} \cos 2\phi_p + \hbar\tilde{v}_{TL'} W^{TL'} \sin\phi_p \right], \quad (1)$$

where ε' and Ω' are the energy and solid angle corresponding to the scattered electron and $\Omega_p \equiv (\theta_p, \phi_p)$ is the solid angle for the outgoing proton. The helicity of the incident electron is labeled by h and σ_M is the Mott cross section. The term κ is given by $\kappa = p_p M_p / (2\pi\hbar c)^3$, with p_p the momentum carried by the emitted proton and M_p its mass. Finally, \tilde{v}_K are the factors containing the dependence on the electron kinematics. These coincide with the kinematic factors v_K in Refs. [13,15] except for $K = TL$ and TL' where $\tilde{v}_K = \sqrt{2}v_K$.

The hadronic content of the problem is contained in the response functions W^K , $K = L, T, TL, TT, TL'$ where L and T denote the longitudinal and transverse projections of the nuclear current with respect to the momentum transfer \mathbf{q} , respectively. These functions are related to the R^K responses in Refs. [13,15] by $W^K = R^K/\eta$, where $\eta = \kappa$ for $K = L, T$ and TT and $\eta = \sqrt{2}\kappa$ for $K = TL$ and TL' .

The five responses in Eq. (1) can be expressed (see Refs. [13,15]) in terms of the matrix elements of the usual Coulomb, electric and magnetic multipole operators, between the ground state of the ^{16}O and the hadronic state $|\alpha\rangle = |lj, J_B; J\rangle$. This represents a proton in the continuum with asymptotic angular momenta lj , coupled with the angular momentum J_B of the residual nucleus ^{15}N to a total angular momentum J . The residual nucleus state is described as a hole in the closed-shell core of the ^{16}O . The corresponding wave function is obtained as a solution for a real Woods-Saxon potential fitted to reproduce the single-particle energies near the Fermi level and the experimental charge density [16]. The outgoing proton wave function is described as a plane wave or as the solution of the Schrödinger equation for positive energies using, either the same Woods-Saxon potential as for the hole states, or a complex optical potential fitted to elastic proton-nucleus scattering data. In this way we can study the sensitivity of the various response functions to FSI.

Finally, the evaluation of the hadronic response functions requires the knowledge of the four-nuclear current operator. Here, for the charge operator we consider the usual approach that includes only the one-body operator corresponding to protons and neutrons. On the other hand, the nuclear vector current includes non-relativistic one-body convection and spin-magnetization pieces and also a two-body part. In particular, for this last two-body component we consider the traditional non-relativistic reduction of the lowest order Feynman diagrams with one-pion exchange and/or isobar excitation in the nucleon intermediate state [17]. This contains the MEC (seagull and pion-in-flight) and IC terms. Thus, our model is similar to that used in previous calculations, except for the unlike procedure followed by Boffi and Radici [7] in their evaluation of the two-body matrix elements, and for the slightly different values of the coupling constants in the IC considered by Van der Sluys *et al.* [8]. The corresponding matrix elements of the multipole operators are the same as the particle-hole ones for the inclusive reaction and can be found in Ref. [11].

In Figure 1 we illustrate the effects of the FSI on the various response functions by showing results corresponding to different approaches. In all the cases, MEC and IC have been included in the evaluation of the responses. Left panels correspond to a proton knockout off ^{16}O from the $1p_{1/2}$ shell, and right panels to the $1p_{3/2}$ orbit. Dotted curves have been obtained in the plane wave (PW) approach for the outgoing proton. Note that, in this case, the electron polarized response $W^{TL'}$ is identically zero. Results corresponding to the continuum shell-model with the same Woods-Saxon potential as for the hole states are represented by dashed lines. Finally, dot-dashed and solid lines correspond to results obtained using the phenomenological complex optical potentials of Schwandt *et al.* (S) [18] and Comfort and Karp (CK) [19], respectively.

As seen in Fig. 1, the main effect of FSI is an overall reduction of the W^T and W^{TL} response functions, whereas W^{TT} is enhanced with respect to the PW result. This effect is particularly pronounced when FSI are described with the two optical potentials. As known, the presence of an imaginary term in the potential produces a significant overall reduction of the cross section and our results show that it also affects the response functions by reducing or enhancing them. It is also interesting to point out that the results obtained for the W^T , W^{TL} and W^{TT} responses using the two phenomenological optical potentials are very similar. On the contrary, the discrepancies are clearly larger in the case of the electron polarized response $W^{TL'}$. The fact that $W^{TL'}$ is only different from zero when FSI are taken into account, makes plausible to expect a larger sensitivity of this response to different FSI approaches.

Comparing the results obtained for the two spin-orbit partner shells, $1p_{1/2}$ and $1p_{3/2}$, one observes that the pure transverse response W^T is very similar in both cases apart from the different occupation factors (twice for the $1p_{3/2}$ hole state). The effects introduced by the various FSI approaches are basically the same for both hole states. In the case of the W^{TT} response, the result for $1p_{3/2}$ has opposite sign to that for $1p_{1/2}$ where moreover, FSI makes the response to change sign compared to the PW result. However, the small strength of this response makes hard to draw any conclusion.

The case of the interference longitudinal-transverse response W^{TL} is particularly interesting. Its strength, much larger than W^{TT} , makes it suitable to be measured with relatively high precision. Furthermore, in some recent papers [13,21] it has been shown that W^{TL} is very sensitive to different aspects of the reaction mechanism such as relativistic approaches to the current and wave functions. From the results in Fig. 1 one observes that the effects of FSI are rather different for both shells. Whereas the use of a complex optical potential reduces significantly the strength for $1p_{1/2}$, on the contrary, this effect is largely suppressed for the $1p_{3/2}$ hole state. Moreover, note that in this last case the results obtained with both optical potentials do not differ too much from the response calculated with the continuum shell-model based on a real Woods-Saxon potential.

The role played by the two-body components of the current can be seen in Fig. 2 where we show the W^T and W^{TL} responses for the two orbits we are considering. Therein, dotted curves correspond to results obtained with the one-body current. Dashed curves include also the seagull contribution. Dot-dashed curves show the full MEC effect, i.e., seagull and pion-in-flight currents. Finally, the solid curves correspond to results calculated with the full current, i.e. including also IC terms. All the calculations in this figure have been performed using the Comfort and Karp optical potential [19]. As we can see, the behavior of the results obtained for the two orbits is similar. The combined effect of both MEC and IC in the W^T response is very small. This agrees with the results obtained for (e,e') processes using the same model [11]. On the contrary, for the interference W^{TL} response we observe an appreciable contribution of the two-body currents, mainly due to the seagull term. In this case, the effect of the IC is practically negligible.

Another point of interest is related to the possible dependence of these results with the choice of the FSI model. In order to study this question we present in Table 1 a systematic analysis of the relative effects of the different terms of the current (MEC and IC) at the peaks of the various response functions for the FSI approaches we have considered in this work.

It is clear from the table that the total MEC+IC effect depends on the model of FSI. In this respect, it is remarkable the fact that when the real part in the potential describing FSI enhances (reduces) the two-body total effect, the addition of an imaginary part diminishes (increases) such effect. This is relevant because the results do not show sensitivity to the particular parameterization used for the optical potential. On the other hand, this cancelation is responsible for the small two-body contribution (at most $\sim 10\%$) found for S or CK optical potentials, except for the $1p_{1/2}$ TL response ($\sim 35\%$), where the imaginary part of the optical potential interferes coherently with the MEC.

In general, the effect due to IC is considerably smaller (in absolute value) than the one produced by MEC and only in some cases (e.g. for the T response) they are of the same order.

Finally, it is worth to mention that the total MEC+IC effect is larger, in absolute value, in the case of the $1p_{1/2}$ orbit than in the $1p_{3/2}$ one. The only exception to this observation appears in the second peak of the TL' response.

Our results disagree in general with those of Van der Sluys *et al.* [8]. These authors predicted for W^T and W^{TL} a strong cancelation of the effects due to MEC and IC in the case of the $1p_{1/2}$ orbit, whereas the strength of the responses for $1p_{3/2}$ appeared to be noticeably increased. Moreover, a huge contribution of the IC was encountered. Only in the case of the W^T response for the $1p_{1/2}$ orbit our results are compatible with theirs. Nevertheless, we must point out that a similar disagreement was already noticed for (e,e') processes [20].

The results of our calculations differ also significantly from those of Boffi and Radici [7] who encountered a large IC effect for W^T , W^{TT} and $W^{TL'}$ corresponding to the $1p_{1/2}$ orbit and for W^{TT} and $W^{TL'}$ in the case of the $1p_{3/2}$ orbit. However, the situation for the W^{TL} response is qualitatively similar to ours for both orbits, though we find a larger effect. Then, the discrepancies observed could be ascribed to the ‘‘approximate’’ procedure followed by these authors to evaluate MEC and IC contributions.

To finish our study, in Fig. 3 we compare our calculations to the experimental data [10] for the W^T and W^{TL}

responses. Therein, solid curves correspond to the full calculation performed using the Comfort and Karp optical potential [19]. The curves have been multiplied by a factor 0.8 for $1p_{1/2}$ and 0.7 for $1p_{3/2}$, needed to bring the calculated T response to experiment. This values differ from the spectroscopic factors considered in previous studies [8,10]. As can be seen, it is not possible to describe simultaneously the two responses. The result for W^{TL} in the case of the $1p_{3/2}$ orbit shows the larger disagreement.

In this work we have tried to disentangle the situation concerning the role played by the MEC and IC in $(\bar{e}, e'p)$ processes. Contrary to what Van der Sluys and coworkers have obtained [8], we do not find any great differences in the results obtained for the two orbits considered. On the other hand, the effect of the IC is in general rather small or, at most, comparable with that due to MEC. A similar situation has also been found in Ref. [22], where the two-body current effects in (p, γ) reactions appear to be small. An extension of our calculations to other nuclei and kinematical regions could help to fully clarify the problem. Work in this direction is being carried out.

ACKNOWLEDGMENTS

This work has been supported in part by the DGICYT (Spain) under contract Nos. PB95-0533-A, PB95-0123, PB95-1204 and by the Junta de Andalucía (Spain).

-
- [1] S. Frullani and J. Mougey, *Adv. Nucl. Phys.* **14**, 1 (1984); S. Boffi, C. Giusti, and F.D. Pacati, *Phys. Rep.* **226**,1 (1993); J.J. Kelly, *Adv. Nucl. Phys.* **23**,77 (1996).
 - [2] J. Knoll, *Nucl. Phys.* **A223**, 462 (1974); J.P. McDermott, *Phys. Rev. Lett.* **65**, 1991 (1990); Y. Jin, H.P. Blok, and L. Lapikás, *Phys. Rev. C* **48**, R964 (1993); Y. Jin, D.S. Onley, and L.E. Wright, *ibid.* **50**, 168 (1994).
 - [3] C. Giusti and F.D. Pacati, *Nucl. Phys.* **A473**, 717 (1987); *ibid.* **A485**, 461 (1988).
 - [4] J.M. Udías, P. Sarriguren, E. Moya de Guerra, E. Garrido, and J.A. Caballero, *Phys. Rev. C* **48**, 2731 (1993); *ibid.* **51**, 3246 (1995).
 - [5] S. Boffi, C. Giusti, and F.D. Pacati, *Nucl. Phys.* **A336**, 416 (1980); C. Giusti and F.D. Pacati, *ibid.* **A336**, 427 (1980); A. Picklesimer, J.W. Van Orden, and S.J. Wallace, *Phys. Rev. C* **32**, 1312 (1985); A. Picklesimer and J.W. Van Orden, *ibid.* **35**, 266 (1987); *ibid.* **40**,y (1989); J. Ryckebusch, M. Waroquier, K. Heyde, J. Moreau, and D. Ryckbosch, *Nucl. Phys.* **A476**, 237 (1988); J. Ryckebusch, K. Heyde, D. Van Neck, and M. Waroquier, *Phys. Lett. B* **216**, 252 (1988); *Nucl. Phys.* **A503**, 694 (1989); S. Boffi and M. Radici, *Phys. Lett. B* **242**, 151 (1990); S. Boffi, C. Giusti, F. Pacati, and M. Radici, *Nucl. Phys.* **A518**, 639 (1990); Y. Jin, D.S. Onley, and L.E. Wright, *Phys. Rev. C* **45**, 1311 (1992); S. Boffi, M. Radici, J.J. Kelly, and T.M. Payerle, *Nucl. Phys.* **A539**, 597 (1992); J.J. Kelly and S.J. Wallace, *Phys. Rev. C* **49**, 1315 (1994); J.J. Kelly, preprint nucl-th/9809090.
 - [6] T. Suzuki, *Nucl. Phys.* **A495**, 581 (1989).
 - [7] S. Boffi and M. Radici, *Nucl. Phys.* **A526**, 602 (1991).
 - [8] V. Van der Sluys, J. Ryckebusch and M. Waroquier, *Phys. Rev. C* **49**, 2695 (1994).
 - [9] L. Chinitz *et al.*, *Phys. Rev. Lett.* **67**, 568 (1991).
 - [10] G.M. Spaltro *et al.*, *Phys. Rev. C* **48**, 2385 (1993).
 - [11] J.E. Amaro, G. Co', E. Fasanelli, and A.M. Lallena, *Phys. Lett. B* **277**, 365 (1992); J.E. Amaro, G. Co', and A.M. Lallena, *Ann. Phys. (N.Y.)* **221**, 306 (1993); J.E. Amaro, G. Co', and A.M. Lallena, *Nucl. Phys.* **A578**, 365 (1994).
 - [12] J.E. Amaro *et al.*, *Nucl. Phys.* **A602**, 263 (1996); J.E. Amaro, J.A. Caballero, T.W. Donnelly and E. Moya de Guerra, *ibid.* **A611**, 163 (1996).
 - [13] J.E. Amaro and T.W. Donnelly, *Ann. Phys. (N.Y.)* **263**, 56 (1998); *Nucl. Phys.* **A646**, 187 (1999).
 - [14] J.E. Amaro, A.M. Lallena, and J. Nieves, *Nucl. Phys.* **A623**, 529 (1997).
 - [15] A.S. Raskin and T.W. Donnelly, *Ann. Phys. (N.Y.)* **191**, 78 (1989).
 - [16] J.E. Amaro, C. García-Recio, and A.M. Lallena, *Nucl. Phys.* **A567**, 701 (1994); S. Moraghe, J.E. Amaro, C. García-Recio, and A.M. Lallena, *ibid.* **A576**, 553 (1994).
 - [17] D.O. Riska, in: *Mesons in Nuclei*, Vol. II, eds. M. Rho and D. Wilkinson (North-Holland, Amsterdam, 1979), p. 752; *Phys. Rep.* **181**, 208 (1989).
 - [18] P. Schwandt *et al.*, *Phys. Rev. C* **26**, 55 (1982).
 - [19] J.R. Comfort and B.C. Karp, *Phys. Rev. C* **21**, 2162 (1980).
 - [20] V. Van der Sluys, J. Ryckebusch, and M. Waroquier, *Phys. Rev. C* **51**, 2664 (1995).
 - [21] J.A. Caballero, T.W. Donnelly, E. Moya de Guerra and J.M. Udías, *Nucl. Phys.* **A632**, 323 (1998); *ibid.* **A643**, 189 (1998).
 - [22] T.B. Bright *et al.*, *Nucl. Phys.* **A603**, 1 (1996).

FIG. 1. Response functions for proton knockout off ^{16}O from the $1p_{1/2}$ (left panels) and $1p_{3/2}$ (right panels) orbits, as a function of the missing momentum. The momentum transfer is $460 \text{ MeV}/c$ and the excitation energy 100 MeV . Dotted lines correspond to PW. Dashed curves correspond to DW using the continuum shell-model based on a Woods-Saxon potential [11]. Finally, dot-dashed and solid curves represent the results obtained with FSI evaluated using the optical potentials of Schwandt *et al.* [18] and Comfort and Karp [19], respectively. MEC and IC are included in all cases.

FIG. 2. W^T and W^{TL} responses for proton knockout off ^{16}O from the $1p_{1/2}$ (left panels) and $1p_{3/2}$ (right panels) orbits, as a function of the missing momentum. Momentum transfer is $460 \text{ MeV}/c$ and excitation energy 100 MeV . The calculations have been performed by means of the Comfort and Karp optical potential [19] to describe the wave function of the emitted proton. Dotted curves correspond to the one-body terms in the current operator. Dashed curves include also the seagull two-body contribution. Dot-dashed curves have been obtained with the full MEC operator. Solid curves take into account MEC and IC.

FIG. 3. The W^T and W^{TL} responses for proton knockout off ^{16}O from the $1p_{1/2}$ and $1p_{3/2}$ orbits calculated with the Comfort and Karp optical potential [19] are compared with the experimental data at a momentum transfer of $460 \text{ MeV}/c$ and an excitation energy of 100 MeV (see Ref. [10]). Solid line represents the full calculation (including MEC and IC) scaled with factors 0.8 for the $1p_{1/2}$ and 0.7 for the $1p_{3/2}$ orbits.

TABLE I. Relative effect of MEC and IC. The values (in %) refer to the peak of the respective responses. The wave function of the emitted proton is described by means of plane waves (PW), an orbit of the continuum shell-model based in a Woods-Saxon potential (CSM) [11] and the optical potentials of Schwandt *et al.* (S) [18] and Comfort and Karp (CK) [19], respectively. The response $W^{TL'}$ is zero in PW (and is omitted) and shows two peaks in the other cases.

		$1p_{1/2}$			$1p_{3/2}$		
		MEC	IC	Total	MEC	IC	Total
T	PW	7.3	-3.7	3.5	4.5	-3.9	0.5
	CSM	2.3	-5.1	-2.8	2.8	-4.7	-1.9
	S	4.7	-4.0	0.6	3.6	-3.8	-0.3
	CK	5.1	-3.7	1.3	3.8	-3.7	-0.1
TL	PW	24.7	0.6	25.3	12.2	-0.1	12.2
	CSM	18.6	1.2	19.9	11.9	-0.6	11.3
	S	32.3	3.3	35.8	8.9	-1.0	7.9
	CK	29.1	2.9	32.2	9.2	-0.8	8.4
TT	PW	-76.3	29.3	-43.8	-22.9	7.8	-13.4
	CSM	58.2	-20.9	32.5	-16.3	1.1	-14.5
	S	19.9	-9.2	9.8	-2.6	-1.7	-4.1
	CK	18.2	-9.3	8.1	-2.1	-1.9	-3.8
TL'	CSM	-192.4	-10.9	-203.9	6.2	-0.6	5.6
		5.1	-2.4	2.4	9.7	-0.7	8.7
	S	9.0	0.8	9.8	3.1	-2.7	0.3
		3.4	-2.6	0.4	7.1	-1.4	5.8
	CK	8.3	2.5	10.7	2.8	-3.0	-0.2
		4.4	-3.2	1.2	8.3	-2.0	5.9

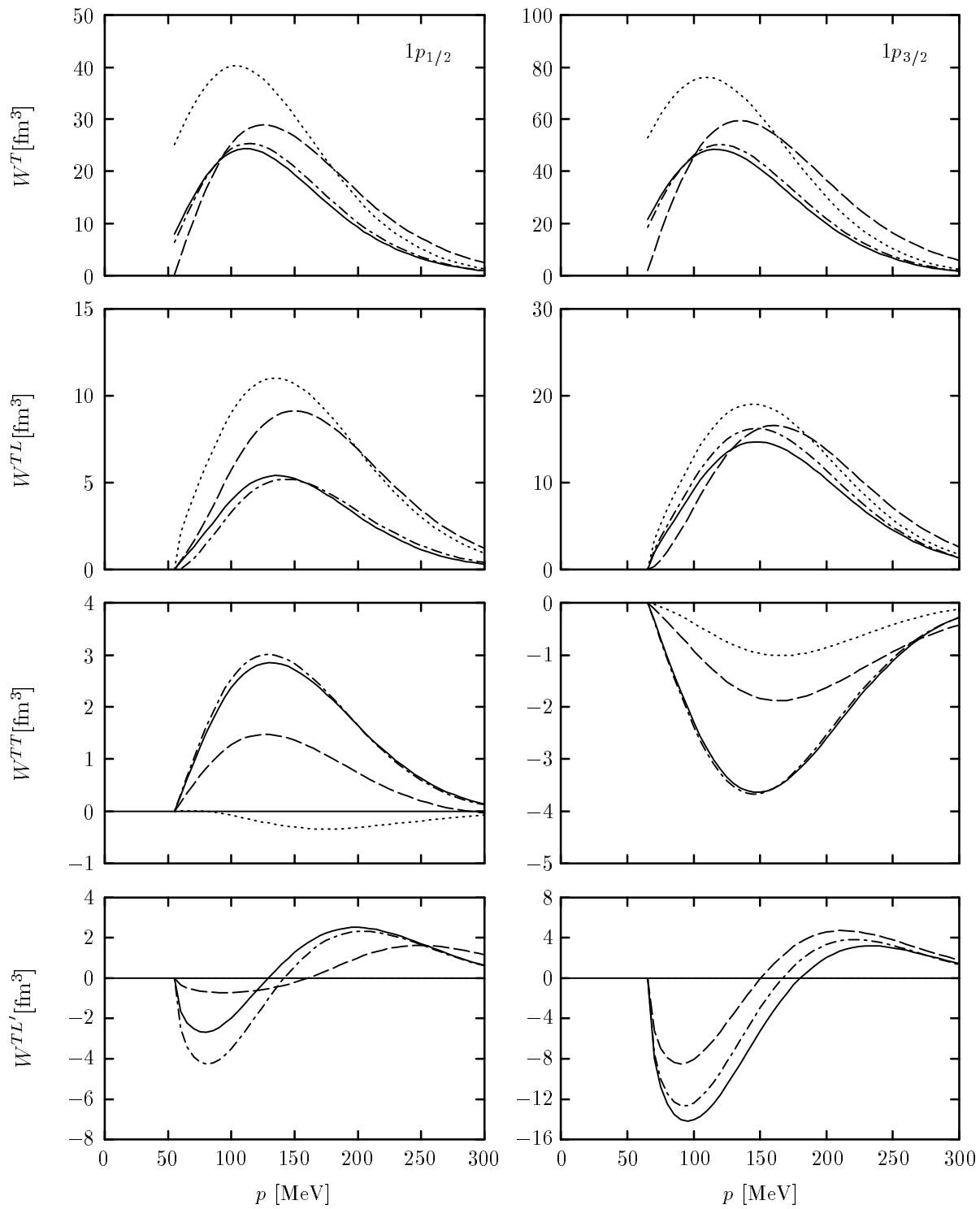


Figure 1

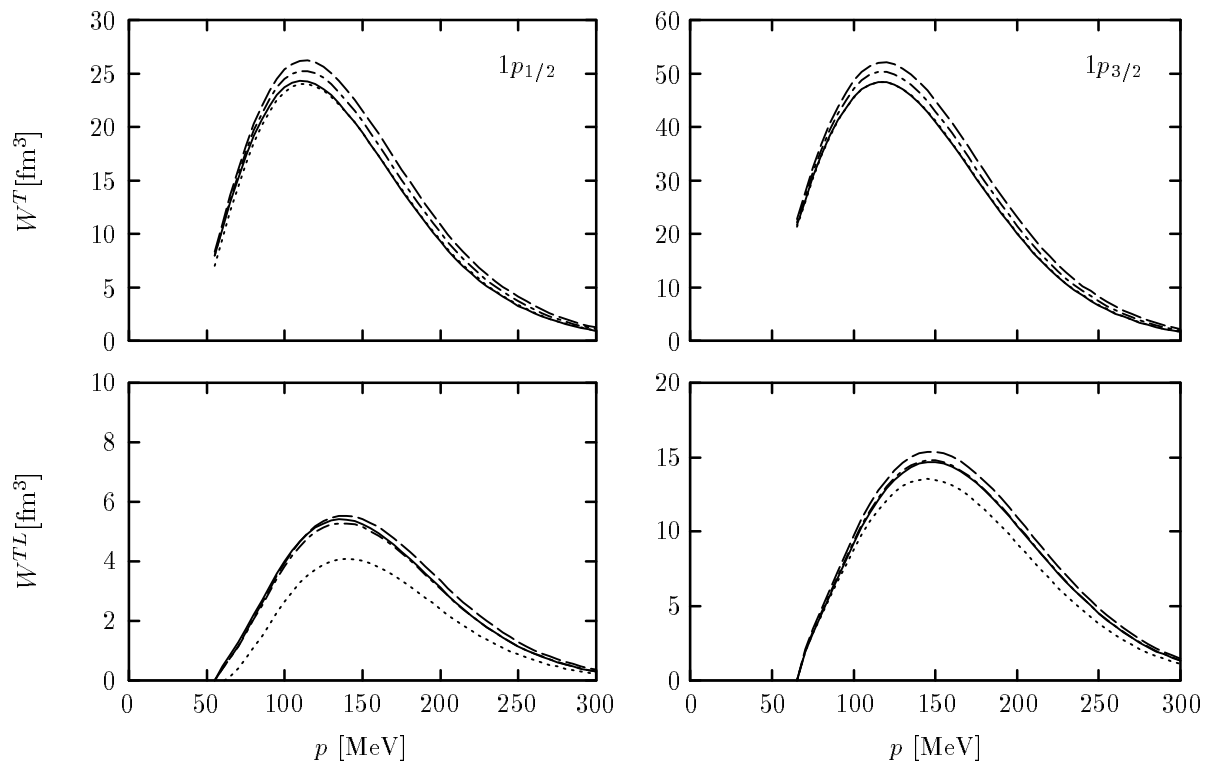


Figure 2

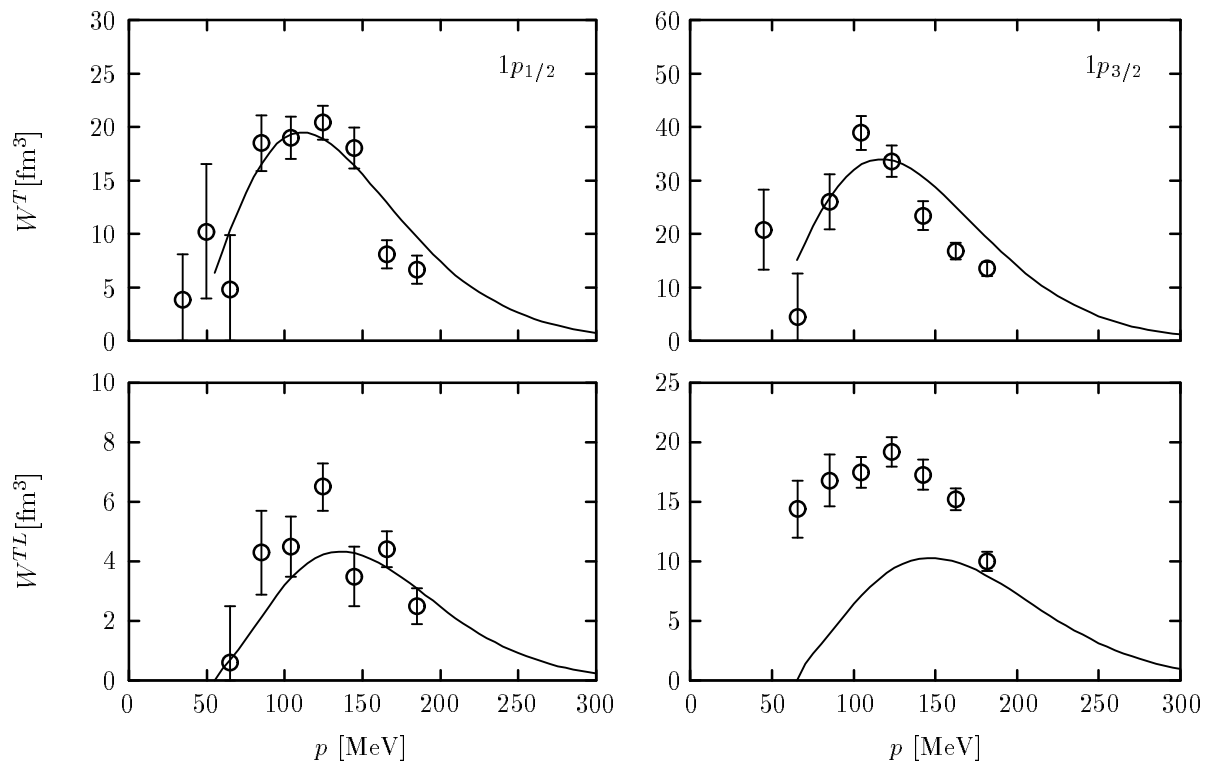


Figure 3